European Space Agency
Directorate of Human Spaceflight and Operations
Ground System Engineering Department
Flight Dynamics Division
Mission Analysis Section

MAS Working Paper No. 571

ECho Mission Analysis Guidelines

Issue 1, Revision 0

by B. De Vogeleer

September 16th, 2011

ESOC European Space Operations Centre

Abstract

The primary objective of the EChO mission is to study the physics and chemistry of the atmospheres of a representative sample of known transiting exoplanets found around nearby stars. The differential technique of transit spectroscopy will be used over the optical to thermal IR wavebands (0.4 to 11/16 micron) to determine the physical and chemical conditions of the atmospheres of a sample of several tens of known exoplanets with masses ranging from Jupiter-, to a few Earth's- size and equilibrium temperatures of 2000 K to 300 K respectively. To achieve this, the scientific requirements involve a high photometric stability, resulting in fine thermal and pointing stability. Additionally, the low noise requirements imply that cryogenic operating conditions are necessary, both for the telescope and the focal plane detectors. The Sun-Earth L_2 point is the ideal environment for this type of mission. The dynamics that create these libration points also enable a more or less stable orbital geometry that satisfies the mission needs: large amplitude quasi-Halo orbits at the night-side Lagrange point (L_2) of the Sun-Earth system. Further advantages are a rather short transfer time and a transfer and insertion free from deterministic manoeuvres, which keeps the propellant consumption very low. This document contains a first partial mission analysis. It is demonstrated that for orbits with a Sun-Spacecraft-Earth angle of $< 34°$ (roughly 1 million km) there is a monthly launch window of up to 25 days in the launch period of 2020-2022, while around the equinoxes there are larger gaps due to the occurrences of Earth-eclipses. The daily launch window lasts between 1 and 2 hours, centered around 12:30 UTC. A sample trajectory is taken and the relevant orbit parameters are elaborated. The orbit maintenance is not analysed due to lack of system design data and therefore taken from reference data (Herschel/Planck). It is expected that the orbit maintenance will be within $6m/s/year$ (3σ plus margin) for the mission lifetime of 5+1 years. A preliminary launch and ascent trajectory is presented for the Soyuz Fregat MT launcher, with the nominal launcher insection conditions: $r_\pi = 335.25\,km$, $e = 0.9906$, $i = 6.061°$, the argument of the ascending node with respect to Greenwhich $\Omega_G = 185.646°$, the argument of perigee $\omega = 180.071°$ and a true anomaly $\theta = 35.015°$ at injection. The launcher performance is assessed and for a direct insertion into a transfer towards L_2 , the launch payload mass is $2145\,kg$, which includes the adapter and margin. The transfer navigation has been simulated numerically and constitutes of the launcher dispersion correction ($44.61\,m/s$, for 99% of the cases) and the perigee velocity correction ($12.6\,m/s$, for 99% of the cases). That brings the total ΔV budget to $93.21\,m/s$, including margins for the mission lifetime. An alternative LEOP scenario with a launch into a highly elliptical orbit, has been documented as well.

Change Record

Date	Issue	Rev.	changes to	remarks
16 September 2011	1	0	all	first release

Document Approval

	Signature	Date
Prepared by:	Bram De Vogeleer	Digitally signed by Bram De Vogeleer DN: cn=Bram De Vogeleer, o=ESA, ou=HSO-GFA, email=Bram.De.Vogeleer@esa.int, c=DE Date: 2011.09.16 16:06:33 Z
B. De Vogeleer (HSO-GFA)		
Approved by:	Florian Renk	Digitally signed by Florian Renk DN: cn=Florian Renk, o=ESA, ou=HSO-GFA, email=Florian.Renk@esa.int, c=DE Date: 2011.09.16 18:02:33 +02'00'
F. Renk (HSO-GFA)		

Distribution

Recipient	Institution
Bram De Vogeleer	ESA HSO-GFA
Florian Renk	ESA HSO-GFA
all MAS staff	ESA HSO-GFA
Ludovic Puig	ESA SRE-PAM
Massimo Palladino	ESA TEC-MSM
Remy Chalex	ESA TEC-SYE

Contents

List of Tables

List of Figures

List of Acronyms and Abbreviations

AOCS	Attitude and orbit constrol system
AU	Astronomical unit
CDF	Concurrent design facility
CReMA	Consolidated report on mission analysis
EChO	Exoplanet characterisation observatory
ESA	European space agency
FOV	Field of view
FP	Flight Program
HEO	High elliptical orbit
MGA	Medium Gain antenna
LDCM	Launcher dispersion correction manoeuvre
LEOP	Launch and early operations phase
LOS	Line of sight
PVCM	Perigee velocity correction manoeuvre
MJD	Modified Julian day
MRD	Mission requirements document
RAAN	Right ascension of ascending node
SAA	Solar aspect angle
S/C	Spacecraft
SSAC	Space science advisory committee
SSCE	Sun-spacecraft-Earth angle
SSCM	Sun-spacecraft-Moon angle
TCM	Trajectory correction manoeuvre
UT, UTC	Universal time

1 Introduction

1.1 Mission Background

The study and search for Exoplanets is of great interest to the science community and EChO (Exoplanet Characterisation Observatory) is an M-class mission candidate for the M3 slot within the Cosmic Vision programme, for a planned launch between 2020 and 2022. EChO, with 3 other science missions, was recommended by the Space Science Advisory Committee (SSAC) to enter an assessment study (Phase 0), starting with an ESA internal study followed by parallel industrial study activities.

The primary objective of the EChO mission is to study the physics and chemistry of the atmospheres of a representative sample of known transiting exoplanets found around nearby stars. The differential technique of transit spectroscopy will be used over the optical to thermal IR wavebands (0.4 to 11/16 micron) to determine the physical and chemical conditions of the atmospheres of a sample of several tens of known exoplanets with masses ranging from Jupiter-, to a few Earth's- size and equilibrium temperatures of 2000 K to 300 K respectively. Transit spectroscopy involves taking differential measurements of in- and out- of transit measurement, which allows to deduce the exoplanet spectrum by subtracting the stellar signal. To achieve this, a high photometric stability is required, resulting in fine thermal and pointing stability. This needs to be controlled over the time interval between 2 measurements that will be used to extract the exoplanet spectrum. Additionally, the low noise requirements imply that cryogenic operating conditions are necessary, both for the telescope and the focal plane detectors. These requirements need to be fulfilled over a mission lifetime of 5+1 years.

The present mission analysis working paper provides the mission analysis guidelines for EChO. It is based on the final report of the EChO CDF study, see [1]. However, during the CDF and in the current document the strong correspondences in spacecraft and trajectory design with Herschel/Planck and PLATO are exploited. These missions, described in [2] and [3], are the blueprints for the mission design for large amplitude quasi-Halo orbits at the night-side Lagrange point (L_2) of the Sun-Earth system.

1.2 Scope of this Working Paper

Mission analysis guidelines are intended as an input to industrial Phase 0 studies being an applicable document to the statement of work. The mission analysis guidelines present a first analysis of basic mission analysis work like orbit selection, launch window computation, and ΔV budgeting. As in every mission analysis there can be some dependencies of the trajectory design decisions on the spacecraft design. However, it is not intended by the mission analysis guidelines to prescribe in any way the spacecraft design decisions, which are to be performed during Phase 0. Rather, the mission analysis will be iterated with the spacecraft design proposed in the industrial phase. In case the presented trajectory design presumes a certain spacecraft design, it should be noted that this does not necessarily represent the optimal solution on the spacecraft side.

1.3 Requirements and Design Drivers

In the Mission Requirements Document from the CDF study, see [4], the main requirements related to mission analysis are listed:

- EChO should be compatible with a Soyuz Fregat MT launch from Kourou,

- Quasi-Halo Orbit around night side Libration point L_2 , such that:
  - Observation duty cycle is feasible
  - Required ΔV budget is reasonable
  - Launch between 2020-2022
  - No eclipses occur during the operational but also during the transfer phase. Both Earth and Moon eclipses have to be avoided.
- The mission has a nominal lifetime of 5 years and all consumables are to be budgeted for the nominal lifetime plus 1 year extension
- Geometrical attitude constraint: at all time the Sun cannot shine directly inside the main telescope aperture. Therefore a minimum angle offset of 20° has to be guaranteed at all times between the sun direction and the telescope LOS. In addition the Earth is also blocked from entering the FOV due to the large albedo and reflection. Important in this context is the maximum attitude excursion from the nominal state. The relevant DOF allows the spacecraft, during the science operations, to tilt 35° towards the Sun, from the nominal state pointing perpendicular to the Sun direction. This constraint is active from the moment of the fairing separation onwards.

From a mission analysis point of view the strongest design drivers are the requirements for a low overall ΔV budget in combination with a feasible launch window.

1.4 Orbits around L_2

Before starting the analysis for EChO, the basic concepts for libration point orbits as established for Planck and Gaia are quickly introduced. The solution of the linearised equations of motion of the circular restricted 3-body problem, in the frame rotating with the minor body (Earth) around the sun, can be written as:

$$\begin{aligned} x &= A_1 e^{\lambda_{xy} t} + A_2 e^{-\lambda_{xy} t} + A_x cos(\omega_{xy} t + \phi_{xy}) \\ y &= c_1 A_1 e^{\lambda_{xy} t} - c_1 A_2 e^{-\lambda_{xy} t} - A_y sin(\omega_{xy} t + \phi xy) \\ z &= A_z cos(\omega_z t + \phi_z) \\ \dot{x} &= A_1 \lambda_{xy} e^{\lambda_{xy} t} - A_2 \lambda_{xy} e^{-\lambda_{xy} t} - A_x \omega_{xy} sin(\omega_{xy} t + \phi_{xy}) \\ \dot{y} &= c_1 A_1 \lambda_{xy} e^{\lambda_{xy} t} + c_1 A_2 \lambda_{xy} e^{-\lambda_{xy} t} - A_y \omega_{xy} cos(\omega_{xy} t + \phi_{xy}) \\ \dot{z} &= -A_z \omega_z sin(\omega_z t + \phi_z) \end{aligned} \tag{1.1}$$

Setting the time t to zero leads to a one-to-one relation between the integration constants of the linear problem:

$$(A_1, A_2, A_y, A_z, \phi_{xy}, \phi_z) \tag{1.2}$$

and the state vector, with

$$A_y = c_2 \, A_x \tag{1.3}$$

where c_2 is a constant (see [5]).

The above set of 6 constants are called Osculating Lissajous Elements. A_x, A_y, A_z are called amplitudes of the orbit. Often the epoch (t = 0) is chosen at y = 0 (crossing of x-z plane in rotating frame), this means $\phi_{xy} = 0$. For small amplitudes the conditions $A_1 = A_2 = 0$ define a Lissajous orbits (both exponential terms suppressed). $A_1 = 0$ defines the stable manifold of a Lissajous orbit. $\phi_z = 0$ or $\phi_z = 180°$ (at $\phi_{xy} = 0$) define orbits with minimum

Earth aspect angle variation for given amplitudes (circular in the y-z plane projection for $A_y = A_z$). The properties of this kind of orbits is further discussed in section 2.1. They are commonly referred to as quasi-halo orbits. Large-amplitude orbits as studied in this note are not at all fully described by above equations, however the state vector to osculating elements transformation can be used to directly see basic properties at that moment, as the amplitudes and also the shape in the $y - z$ plane.

From above equations a condition can also be derived on manoeuvre directions which do not affect the stability ($A_1 = 0$), or orthogonal, with an effect on the stability alone, not changing any other orbital properties (see [5]). This is the basic concept used to construct non-escape orbits around the libration points, also for the non-linear problem, by fixing a direction in space a simple bisection in the velocity will calculate correction manoeuvres and generate the orbits.

For a direct transfer (without lunar gravity assist) to L_2 there is only one solution if the perigee radius vector and the orbit plane (inclination, argument of perigee, right ascension of the ascending node, perigee altitude) are fixed, at least if the perigee is within $\pm 45°$ from the sun direction at that moment. A bisection in the modulus of the perigee velocity then leads to this unique *fuzzy boundary* orbit. If the spacecraft remains on this orbit, without any further manoeuvre, it is called a transfer to a freely reachable non escape orbit around L_2 . The freely reachable orbits in general have large amplitudes.

The freely reachable orbits usually are well suited for observatory mission (Herschel, JWST, and also EChO) whereas the small amplitude orbits, requiring an insertion manoeuvre, are necessary for survey missions, using spin-scanning spacecraft. The minimum ΔV insertion manoeuvre to the orbits with smaller amplitudes will be about 100-120 days from launch (slow transfers), the required ΔV will be of the order of 10 m/s per degree of size reduction (size is a measure for the maximum Sun-spacecraft-Earth angle, related to the root-sumsquare of the A_y and A_z amplitudes). The minimum size of the freely reachable orbits is around 30°. Another local minimum in ΔV for size reduction exists for transfer times around 30 days; this gives the fast transfers.

2 Free-Transfer Large-Amplitude Orbits around L_2

For EChO a free-transfer large-amplitude orbit around L_2 has been selected [1] as the operational orbit. The choice is based on the requirement to reach the operational orbit with a minimum ΔV in combination with the proposed attitude and communication strategy of the spacecraft. The minimum ΔV is warranted by one of the most important characteristics of large amplitude orbits around the near Earth Lagrangian points: the large-amplitude orbits provide a stable manifold that extends to low values of the perigee radius and allows to avoid any deterministic transfer manoeuvre of the spacecraft. Some other advantages over more traditional types of orbits are:

- Science operations can start quickly due to short transfer duration
- Low orbit maintenance budget, science interruption of once a month
- Very stable thermal environment
- Low level of perturbations
- Acceptable launcher performance with Soyuz-MT.

As EChO is designed for the observation of an extensive list of known exoplanets rather than for an all-sky survey, the spacecraft has to remain in an inertial pointing for extended periods of time. This observation strategy makes the exploitation of fixed Sun-Earth geometries, like was done for the Planck mission, impossible. There are two different approaches from the point of view of the system design: the first is that the on-board antenna has to be flexible enough to point towards the Earth depending on the spacecraft attitude within the prescribed envelope of the observation attitude. The other approach is to design the communication system such that the required downlink time does not violate the scientific duty cycle. In that situation it would be feasible to have a fixed body mounted antenna and re-orient the spacecraft such that a link with the ground station can be established. The required contact time is logically a function of the data collection rate and the downlink rate, which then becomes the driver for the communication sytem design. This concept is currently assimilated in the CDF spacecraft design. The relatively large variation of the Sun-spacecraft-Earth angle that can be encountered on a large-amplitude libration orbit is therefore not a strong constraint, but the design of the communications system would benefit, if the variation of this angle is limited.

In the first section of this chapter the characteristics of the large-amplitude libration orbits around L_2 relevant for the mission design are discussed. This is followed by the presentation of the launch window and the orbit parameters for a sample trajectory.

2.1 Properties of Reached Orbit

In order to visualise the properties of the free-insertion orbits as a function of launch date, a sample of trajectories reached without deterministic manoeuvre is shown. The lack of transfer manoeuvres restricts the degrees of freedom for changing the orbits characteristics to the freedom of choosing the state at injection, which is determined by the launch time and date (see section 2.2). The geometrical shape of the target orbits is best shown in the projection of the trajectory to the plane perpendicular to the Earth-Sun line. This plane is fixed in the frame that rotates with the Earth around the Sun. Therefore the frame with the origin in the Earth-Moon barycentre and the x-axis pointing towards the anti-Sun direction (i.e. L_2 lies on the positive x-axis at a distance of approximately $1.508\,10^6\,km$) is chosen for

visualisation. The y-axis is chosen so that the $x-y$ plane is the ecliptic. Then, the projection of the orbit to the $y-z$ plane represents the trajectory as seen when viewed from the Earth towards L_2. In figure 2.1 the projections of the trajectory in the $y-z$-plane of the co-rotating

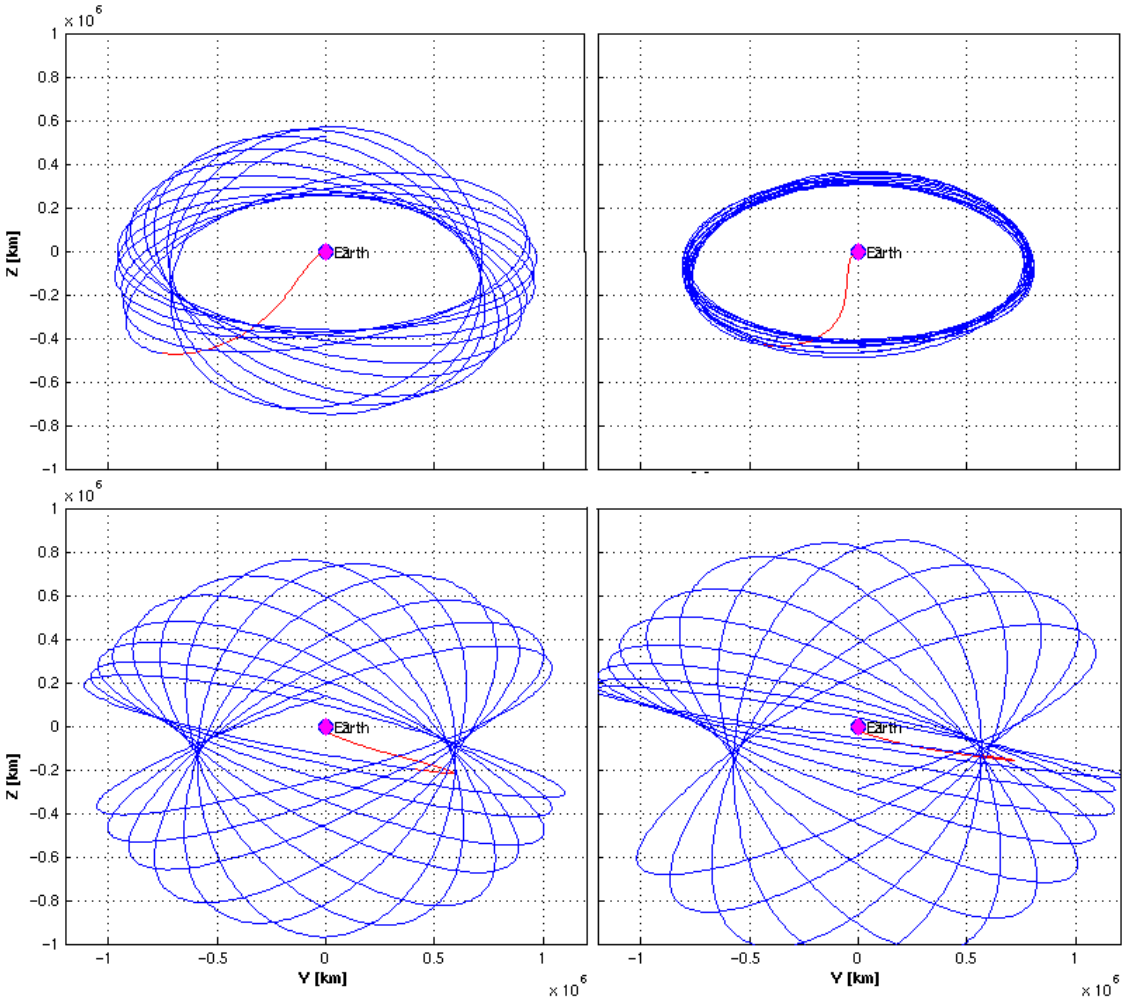

Figure 2.1: Sample of L_2 orbits projected on the $y-z$ plane of the co-rotating frame, following an optimal Soyuz Fregat MT launch on 1-1-2021, as a function of launch hour: at 11:30UT (upper left), 12:30UT (upper right), 15:30UT (lower left), 16:00UT (lower right).

coordinate frame are shown for various launch dates and times. The four cases of trajectories are chosen to illustrate the geometric properties of a sample orbit around L_2. The example of a launch on *2021-1-1 at 11:30UTC* shows a trajectory that exhibits a relatively large variation in the Sun-spacecraft-Earth angle. This trajectory resembles a Lissajous orbit, only that it is much larger and changes its amplitudes. Due to the launch around the solstice time, the initial transfer has a relatively large out-of plane component. For a launch only 60 minutes later on the same day a trajectory very close to the halo condition is found (upper right). For these quasi-halo orbits the in- and out-of plane libration frequencies are very close and the amplitude does not change much. As a consequence, quasi-halo orbits exhibit a relatively small variation in the Sun-spacecraft-Earth angle. This shows that near the halo condition there is a whole family of quasi-halos, since the actual halo condition was not introduced as a constraint for the launch at *12:30 UTC*. Further away (in launch time) from the quasi-halos the motion may be rather perturbed, changing class between large amplitude Lissajous and

quasi-halo arcs. For example a launch at *15:30 UTC* and *16:00 UTC* on the same day leads to an orbit very distinct from the quasi-halo. The latter case is very close to exhibiting an eclipse during the 5+1 year mission. A final type of orbits, not shown here, occurs when the launch takes place around the equinoxes. Then, the apsis line of the transfer lies closer to the ecliptic plane with a potential for eclipses during that phase of the mission. For later launches on the same day the transfer comes progressively closer to the Earth's shadow as will be shown in the discussion on the launch window in section 2.2. The described borderline case is also of the orbit class that changes between quasi-halo and Lissajous-like behaviour, which is commonly referred to as a hybrid orbit.

2.2 Basic Launch Window with Soyuz Fregat MT

2.2.1 Trajectory Types and Eclipses

From the beginning of the CDF study it was established that the EChO spacecraft and mission had to be compatible with a Soyuz Fregat MT from Kourou, see [4]. Due to the added complexity in the analysis and the corresponding performance loss, all efforts were focused on the single boost launcher scenario. In the case of the two boost scenario of the Fregat upper stage the spacecraft stack is placed in a parking orbit with a first manoeuvre, followed by a coast arc of variable duration and the second manoeuvre to inject the spacecraft in the transfer towards L_2 . The manoeuvre split implies that one can choose the argument of perigee of the transfer, which relaxes the constraints on the launch window. The downside of such a scenario is that this additional degree of freedom is expensive in terms of payload performance. No constraint violations were found that would require the restart capability of the upper stage. Additionally, the single boost launch will result in a more conservative and higher constrained launch window than the generally more relaxed window resulting from a 2-boost sequence, which justifies its selection for the early mission analysis.

The recontruction of an optimum mass performance launch resulted in a low inclined orbit for EChO of about 6°. Using the most conservative figures and applying the appropriate margins as in [6] a launched mass of 2145 kg, including any adapters is available. The launcher performance is discussed in more detail in section 3.1.2.

Figure 2.2 presents the full, transfer-eclipse-free launch window, while focussing on only the relevant information: all launch opportunities of the window 2020-2022 that result in a transfer towards an orbit around L_2 that are free from eclipse for at least 5+1 years. As one can see the y-axis is pruned before 09:00 and after 16:30 UTC: outside the presented contours there are only L_2 -orbits with an amplitude of $> 1.2\ 10^6\ km$. The blue bands indicate the manifestation of an Earth eclipse during the operational phase of the mission. Here only Earth-eclipses are considered. the Moon-eclipses will be added later, but from experience in other missions, the impact on the launch window will be minor. The colourscale indicates the maximum Sun-Spacecraft-Earth angle (SSCE), which is a measure of the size of the operational orbit (the darker, the smaller) and shows two important features. Firstly, that the lowest amplitude orbits are only reachable during small daily launch windows that are centered around 12:30 UTC. Secondly, that the launch window almost closes completely for SSCE angles of $< 31°$, with small periodical windows of 60 minutes per day around the equinoxes. The block-out dates and times due to eclipses during the mission lie naturally close to the launch hours corresponding to bigger ranges in Sun-spacecraft-Earth angle. This is due to the fact that these two conditions are caused by the same geometric property of the orbit: its initial proximity to the ecliptic plane. Halo orbits require a prescribed ratio of in- and out-of ecliptic plane amplitudes. This ratio is determined by the initial conditions

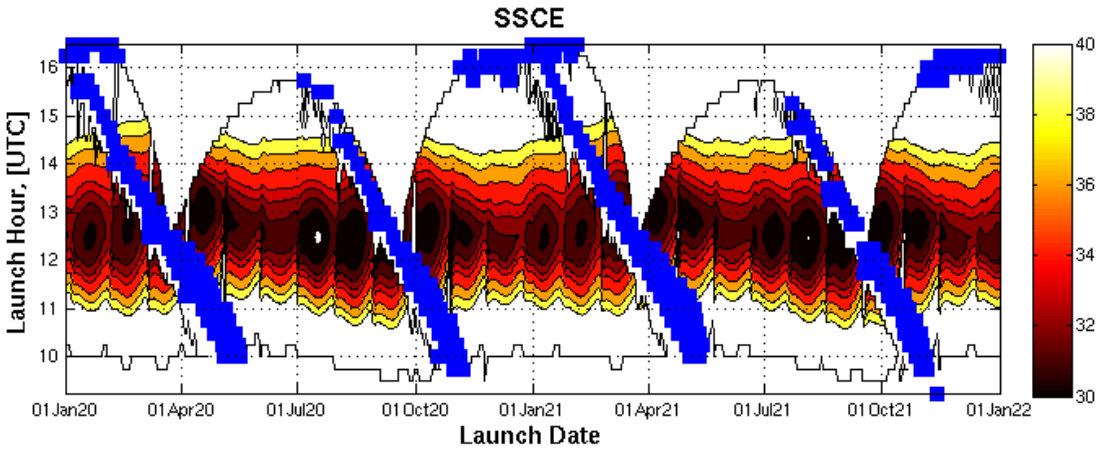

Figure 2.2: Basic transfer-eclipse-free Launch window for EChO from Kourou with a Soyuz Fregat MT. It spans from Jan 2020 to Dec 2021 and assumes a maximum performance launch with a departure inclination of 6.1°. The blue data indicates where an eclipse occurs during the operational phase of the mission. The contour lines represent the size of the operational orbit starting from dark-brown (30°), through red (34°) up to white (40°).

and depends on the declination of the line of apsides of the transfer, which is a function of launch date and time. Orbits starting near the ecliptic will have a strong coupling of the out-of plane component due to their large in-plane amplitude and the violation of the halo condition. This coupling leads to a large variation in the Sun-spacecraft-Earth angle. Transfer eclipses typically occur for late launches (after 14:00 UTC, after the equinoxes), because then the transfer path crosses the anti-Sun direction on the way to L_2 .

2.2.2 System Design Constraints

Apart from these trajectory related constraint there is an aspect of the spacecraft design that also may affect the launch window. The absence of a *mirror-cover* or *shutter mechanism* before the optical train may create a vulnerable situation in case the *Trajectory Correction Manoeuvres* (TCMs, see section 3.4 and 3.5) have to slow the spacecraft down. Although at this stage the thruster configuration is not known, it is hypothesized that the thrust direction is roughly aligned with the LOS of the telescope. Then the spacecraft would need to slew 180° and thrust in the tangential direction of the trajectory. Considering the satellite moves towards L_2, generally in the anti-Sun direction, this may lead to the Sun directly entering the telescope view. To prevent the Sun from entering the forbidden attitude, the launch window could be constrained. In case an accelerating manoeuvre is required, logically there is no risk of violating this constraint. If this constraint would be taken into account, the resulting launch window is presented in the top figure 2.3 and its impact can be summarised as follows, see also section 3.5 for a quantification:

- A preference towards larger amplitude orbits,
- A high rejection rate for daily launch hours after 13:30 UTC. The percentage ramps up from 5% to $> 90\%$ after 14:15 UTC.
- The orientation of the LOS with respect to the Sun at the time of fairing separation must not violate the forbidden attitude constraint. That implies that early launches (before roughly 11:00 UTC) are also discarded.

During the CDF study it was concluded that mechanical or electronical steering mechanisms for the medium gain antenna (MGA) are not the preferred option, as long as a fixed body-mounted antenna can fulfill the observation duty cycle and observation efficiency requirement. This fixed body-mounted antenna implies performing a re-orientation of the complete spacecraft to establish ground contact. For this situation the communications and AOCS design would benefit from an optimised antenna placement and orientation. Something that is benign for the system design, by default is a *minimal variation of the SSCE angle* over the mission lifetime. As an illustration of the importance of this value: consider the quasi-halo orbit around L_2 and assume that the LOS of the telescope is continuously pointing away from the libration point. Then the satellite would rotate 360° per revolution around its x-axis (pointing towards the Sun). If the MGA would be placed on the Sun-side of the spacecraft with a fixed cant angle of $(max(SSCE) + min(SSCE))/2 = 20°$ and a beam width of $max(\Delta SSCE) = 20°$ (half cone angle of 10°), the Earth would constantly be in view of the spacecraft antenna. Since the initial assumption about the attitude is not granted yet, because an observation strategy is not developed yet, it is impossible to optimise this, nor determine a cant angle for the antenna, nor determine the necessary beamwidth. This $\Delta SSCE$ is exactly the parameter that is represented in the bottom of figure 2.3 and is identified as currently one of the two major design drivers for the launch window. From the mission point of view, the size of the orbit is not constrained, altough for SSCE angles of $> 34°$ it becomes harder to impose the quasi-halo condition and then eclipses are more likely to occur somewhere during the mission lifetime. For orbit that are considerably larger than that the orbit maintenance becomes expensive due to the inherently unstable character of the colinear Libration points. If the quasi-halo criterion is lost, the maximum difference in SSCE during the science phase will increase more and leads to complications for the communication system design. The orbits are therefore constrained to $SSCE < 34°$ (see [4]) from a practical point of view, not from the mission analysis. The other driver is being free from eclipse during the nominal mission lifetime plus 1 year of extension.

2.3 Orbit Parameters

From the different types of L_2 orbits as sketched in figure 2.1, the quasi halo (upper right) orbit seems to fullfil the mission needs at best. This is due to the similarity of the in- and out-of-plane oscillation frequencies that cause the SSCE angle to be as constant as possible, simplifying the communication system design. In this section a feasible mission is elaborated as an example of such an operational orbit with launch on 14-04-2021 at 13:57 UTC. Its trajectory has been included in figure 2.4. The maximum amplitude is about $800,000\,km$. The complete transfer takes about 104 days, until the spacecraft reaches the final orbit (blue dot and 'EChO'-label in the Quasi Halo orbit), after which operations can commence. However, 30 days after launch (red part of the transfer) the spacecraft is already in the vicinity of L_2 . The location of the exemplary Day 2, 5 and Day 10 manoeuvres are also indicated with green markers. An optimum performance launch has been assumed, which for a Soyuz launch from Kourou constrains the maximum inclination due to the re-entry of the 3^{rd} stage off the African coast. For EChO a launch nearly East was assumed, leading to a close to minimum orbit inclination. Further, the argument of perigee, right ascension of the ascending node and elapsed time to orbit insertion are also fixed for the direct insertion scenario. Figure 2.5 shows a typical time evolution of the relevant geometrical parameters corresponding to the trajectory of figure 2.4. The important figures are in order of the plot: the declination, the distance to Earth and Moon and the Sun-Spacecraft-Earth/Moon angle. From the upper plot it can be seen that the *declination* for the quasi-halo orbit varies between +30° and -30°, which causes episodes of short daily visibility at the ground-station in Cebreros (+40° latitude). The illustrated periodical behaviour is a characteristic of quasi-halo orbits due to

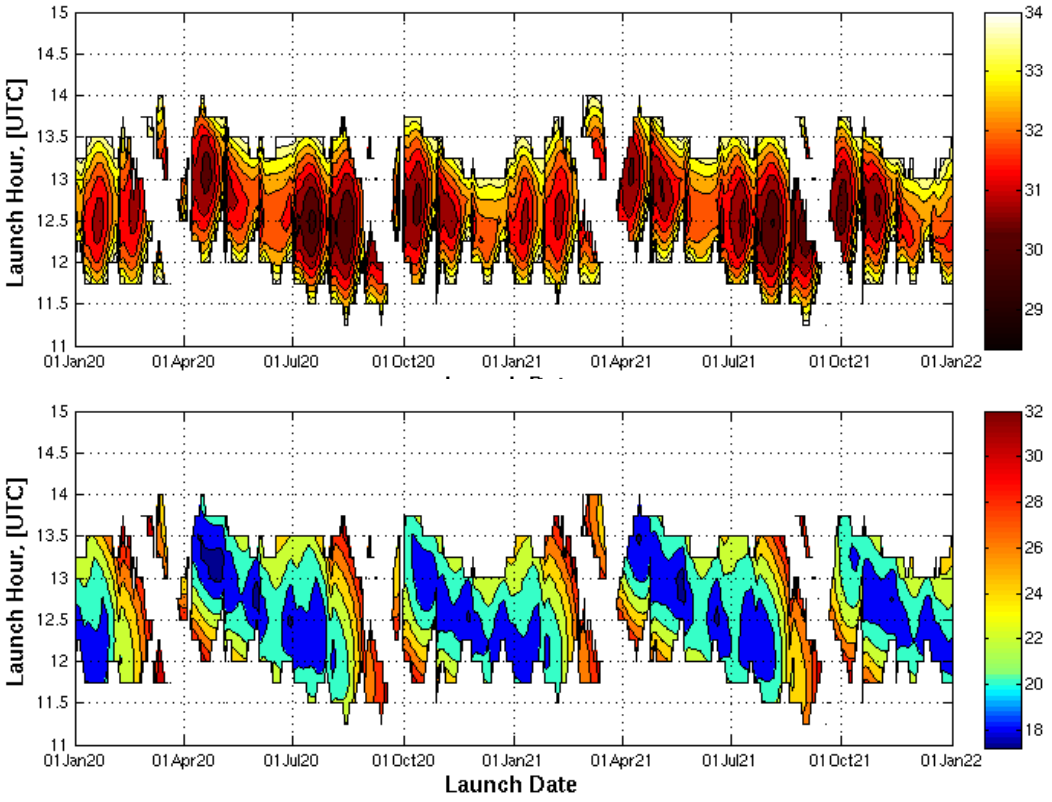

Figure 2.3: Top: The maximum SSCE during mission lifetime and bottom: the difference between maximum and minimum SSCE angle of the operational orbit as a function of the launch date and hour. The SSCE is truncated above $34°$, but trajectories with eclipses are pruned and the thrust direction is constrained.

the halo-condition, which requires a minimum out-of plane amplitude of around $400,000\,km$. For this specific launch date and time, the declination is on average during the winter period lower (and higher during the summer) than the overal average (close to, but different from 0), an obvious consequence of the tilt of the Earth rotational axis. The periodicity is kept due to the orbital period of approximately 180 days or close to half a year. The x-coordinate of the figure represents the summer and winter solstices through the 5+1 years of mission lifetime.

The distance to the Earth varies between $1.2\ 10^6$ and $1.7\ 10^6\ km$. Again the periodical behaviour is very clearly indicated and shows a 2:1 ratio between the orbital period of the spacecraft and the Earth.

The *SSCE angle* is important, since it defines the preferred pointing direction for the solar panels of the spacecraft. For L_2 , Earth lays in the same hemisphere as the Sun, from the spacecraft perspective and therefore, if body mounted solar cells are used, the communication system is placed on the same side of the spacecraft. The SSCE angle then defines the difference in pointing direction between the Earth and the Sun. For the presented quasi halo trajectory the SSCE is at most $31.45°$. The variation of the Sun-spacecraft-Earth angle is minimal ($17.88°$). For this example the quasi halo criterion is imposed: resulting in the the circularity of the quasi-halo orbits. One could find smaller amplitude orbits, but then the quasi-halo criterion is lost, the maximum SSCE variation will be considerably higher and the orbit will behave in a very different manner over time.

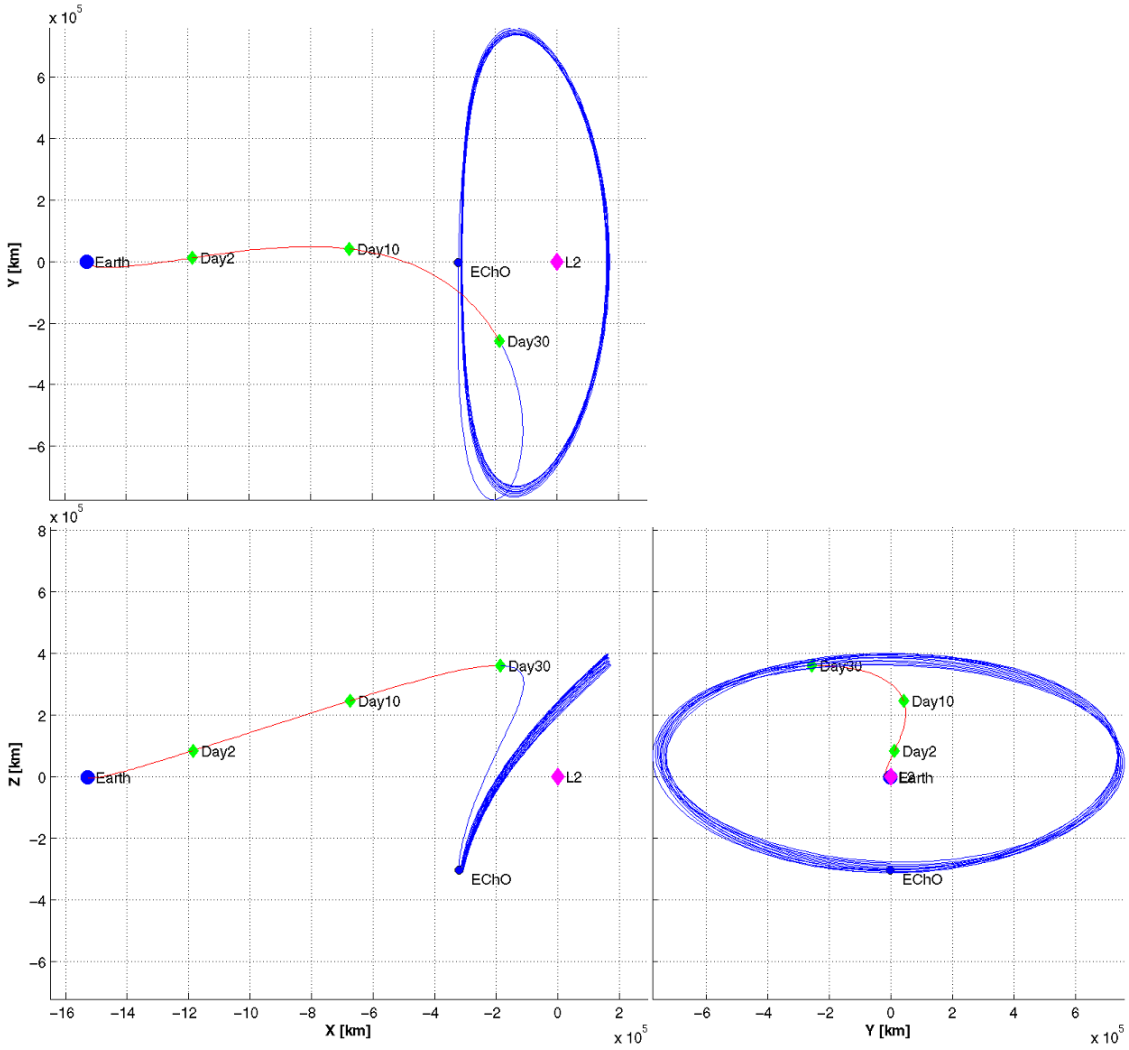

Figure 2.4: Example trajectory for EChO. The trajectory is shown in a synodic reference frame (co-rotating with the Earth's motion around the Sun) with the origin in L_2 , the X-axis pointing towards the anti-Sun direction and Z-axis perpendicular to the Ecliptic plane. The markers show the nominal location for the TCM1, TCM2 and the end of the transfer phase.

A final interesting parameter may be the *Height above Shadow* (the separation from the Earths penumbra, illustrated by the exclusion zone around the anti-Sun direction), but from the trajectory plots (see the y-z projection of figure 2.4) it becomes already clear that for this example trajectory the spacecraft stays at a safe distance from the Earth-Sun penumbra, again a distinguishing property from the quasi-halo orbits. If the launch time is delayed and no corrective actions are undertaken, then the spacecraft will end up in another type of L_2 orbit and eclipses will occur, depending on the initial in- and out-of-plane phase angle. In some cases those phase angles can be chosen to delay the eclipses until after the 5+1 years.

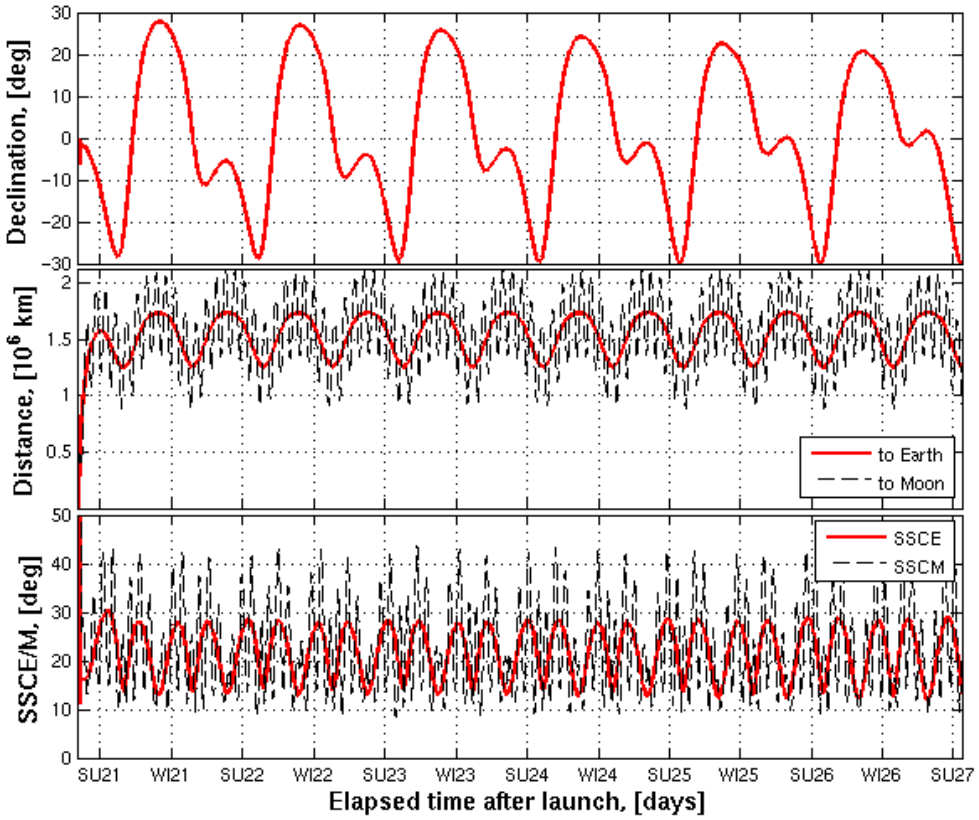

Figure 2.5: Evolution of Mission parameters: declination, SSCE and SSCM, distance to the Earth and the Moon for trajectory with launch on April 14th, 2021 at 13:57 UTC.

2.4 Orbit Maintenance

As a direct consequence from the dynamics that create the libration points, the colinear points represent unstable equilibrium points. Since the EChO-spacecraft would be revolving at a finite distance around L_2 several contributions cause a drift from the reference orbit. Libration missions are particular since the guidance and control does not have to bring the spacecraft back to the reference orbit, which would be more costly than the current approach. Therefore there is no *reference orbit* as such. Instead the idea is to find a new bounded orbit around L_2 , by removing the velocity component that causes the spacecraft to drift away into the unstable manifold. During the operational phase there will be periodic manoeuvres to control the orbit. Although there is a manoeuvre scheduled at apprixmately a monthly interval, they are only executed if the required correction exceeds a certain threshhold value.

For a reliable numerical simulation of this analysis a large amount of data needs to be available or assumed concerning the measurements, ground stations, visibility (antenna design and attitude model), propulsion and AOCS design, etc. The volatility of the data does currently not justify the investment of the effort to analyse a problem that can be roughly covered by applying conservative margins.

Another effect having an influence on the ΔV is the balancing of the thrusters. A balanced system aligns the thrust directions such that parasitic ΔV during attitude manoeuvres (e.g. wheel off-loading) is reduced to zero. In other words, a balanced thruster configuration can provide pure torques without affecting the velocity vector of the spacecraft. Although it

is attempted to minimise the parasitic ΔV for the moment being, the unbalanced thruster configuration with spherical capability will be the starting point for the budget estimate of the orbit maintenance. This system is achieved by mounting the thrusters with a fixed cant angle from the spacecrafts X-axis. With the X-axis aligned with the Sun, the spacecraft only needs to pitch to point the thrusters in the ecliptic plane. Once in the ecliptic, a roll manoeuvre should align the thrust vector with the unstable direction. This configuration is very similar to the one used on Herschel.

The allocated station-keeping budget is therefore taken in accordance with the Herschel mission ($6\, m/s/year$, worst case, comparing to PLATO and Gaia, augmented with a margin according to [6]. This leads to a nominal station keeping ΔV budget of 36 m/s for the minimum mission lifetime of 6 years, to be delivered in the unstable direction. The orbit maintenance cost is given in geometric ΔV not embed any assumptions on the thruster decomposition, which would translate into effective ΔV and propellant mass.

3 Transfer Design

3.1 Launch and Early Ascent

The launcher and launch site were fixed through requirements, so no launcher trade-off was made. However, for the launcher injection strategy, different options exist: launching directly towards L_2 , or using a parking orbit and then use the spacecraft's propulsion system for the injection into the L_2 transfer orbit. The former is chosen as baseline, while the latter is omited in the body of the report and described in appendix A. The performed analysis related to the launcher was limited to the calculation of the launcher performance, simulation of the launcher ascent trajectory, deriving the nominal insertion orbit conditions and definition of the launcher flight program. Section 3.1.1 will sketch the chronological sequence of events that take place during launch, whereafter the following sections will go into more detail. Section 3.3 does the same for the transfer, after which the relevant manoeuvres during the transfer phase are elaborated, including a more detailed analysis for the transfer navigation.

3.1.1 Mission Event Sequence during Launch

Table 3.1 presents an overview of the series of chronological events during a single boost Soyuz Fregat MT launch. The data is taken from the official Arianespace data for the Lunar Lander mission: Next Moon. There the direct injection into a transfer towards L_2 was also investigated. At this stage, the contents of the table serve as a mere illustration of what is going on and the numerical values will be subject to changes as the maturity progresses. Figure 3.1 gives an impression of the ascent trajectory.

Table 3.1: Sequence of events during launch.

Elapsed Time from Lift-off	Comment
L + 8 s	Beginning of pitch motion and first guidance law
L + 15 s	Atmospheric flight at zero angle of attack
L + 118 s	1st/2nd stage separation
L + 213 s	Fairing jettisoning
L + 286 s	Core stage engine cut-off
L + 287 s	3rd stage ignition and 2nd/3rd stage separation
L + 294 s	Tail section jettisoning
L + 558 s	Third stage engine cut-off
L + 561 s	Nose Module separation
L + 621 s	FREGAT main engine ignition
L + 1679 s	FREGAT cut-off
L + 1689 s	Satellite separation Fregat upper stage disposal

3.1.2 Launcher Performance

The launcher performance describes the mass that the launcher can insert in a predefined orbit. In case the orbital plane and the in-plane orientation of the orbit are fixed the only free parameter is the energy of the orbit. For that reason the apogee radius is used as the

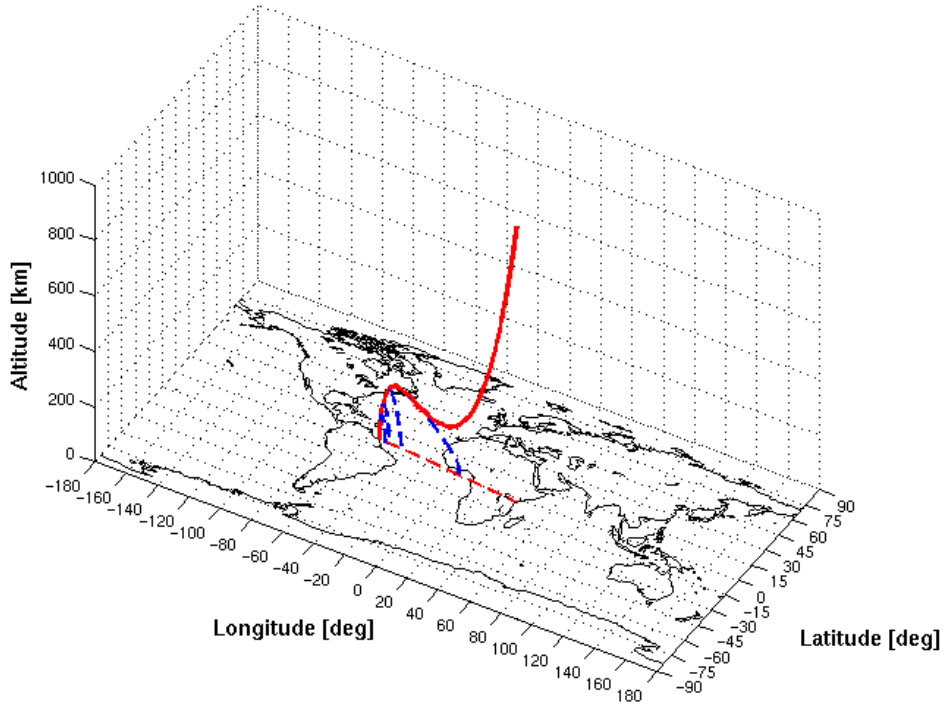

Figure 3.1: Soyuz Fregat MT ascent trajectory for a direct L_2 transfer injection from Kourou without intermediate parking orbit. Z-axis is not to scale.

independent variable. For a direct injection into a transfer towards L_2 the apogee radius amounts to roughly $1.42\,10^6\,km$. The launcher performance is derived from two sets of data. Due to the different sources of information, different margins are applied in accordance with [6]:

- Arianespace data, generated in the frame of the Lunar Lander feasibility study: this results from a highly constrained opimisation and results in conservative, but guaranteed minimum performances.
- Internal software: results from a highly customised optimisation for given payload masses. The software has been validated for mission as PLATO, Gaia, and many more.

The performances for the direct insertion are respectively 2145 kg and 2184 kg for the Arianespace and internal data. Note that these performances are including the payload adapter and also margins. From other missions as Gaia it is known that the final, optimised performances are higher. However, in the end the mass performance contracted with Arianespace is the relevant figure. The possible performance loss due to the Fregat disposal is not reflected in the following performance curve, see 3.1.5.

3.1.3 Nominal Insertion Conditions

For EChO an optimal performance launch is assumed that inserts the spacecraft directly in a transfer towards L_2 . The design of the Soyuz rocket and its stages is such that for single boost launches without coast arcs into higher inclined orbits, the available propellant cannot be completely used. If the burn duration would be longer or a higher transfer inclination

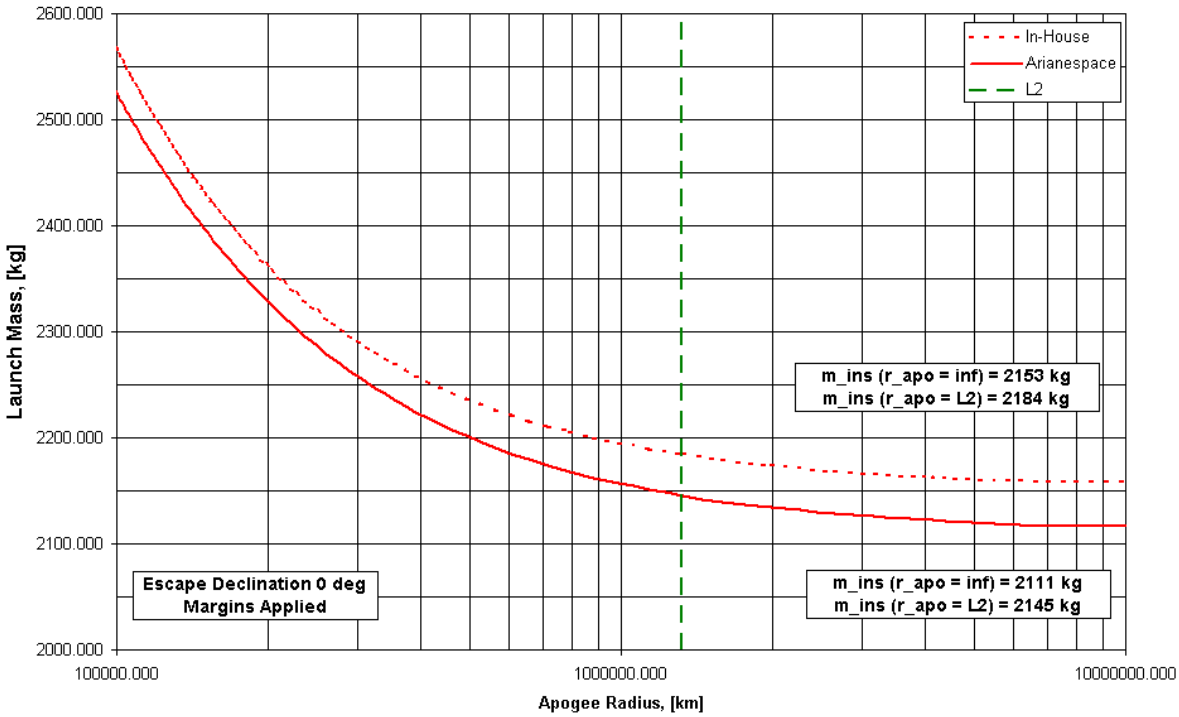

Figure 3.2: Soyuz Fregat MT Launcher performance at separation as a function of the final apogee height.

would be aimed at, the risk for human casualties due to the third stage re-entry would increase too much. However, exploiting the geographical features of the African coastline, for low (close to minimum) inclinations, this problem does not occur. This is also illustrated by the re-entry path of the third stage of the Soyuz rocket in figure 3.1. For that reason a low inclined orbit has been chosen. The other orbital parameters result from an internal optimisation process that reproduced the available Arianespace information very closely in terms of orbit injection parameters. The consequences of assuming an optimal launch in combination with the launcher, launch site, single boost Fregat scenario fixes the following parameters:

- Total burn duration and therefore time to injection
- The azimuth angle at launch and therefore the inclination
- The longitude of the ascending node
- The argument of perigee
- The true anomaly at injection

In addition, for a given flight program the targetted apogee radius of the insertion orbit will also be fixed. Consequently, through fixing the perigee altitude in combination with the other orbital elements, also the eccentricity is frozen. This leads to a situation in which the only degree of freedom is the transfer design is the *Right Ascension of Ascending Node* of the orbit in the inertial reference frame. The RAAN is a function of the date, longitude of ascending node (fixed by ascent trajectory in the rotating frame), but most importantly

the time of launch. The difference in performance between both data sets does not affect the injection conditions, only the amount of payload that is delivered. Table 3.2 presents the parameters of the injection orbit after the Fregat cut-off. Note that Ω_G represents the longitude of the ascending node (therefore in the equatorial plane of the rotating frame) with respect to Greenwich.

Table 3.2: Nominal orbital parameters of the insertion orbit after Fregat cut-off.

Parameter	Units	Nominal Value
Perigee Altitude, r_π	[km]	335.25
Eccentricity, e	[-]	0.9906
Inclination, i	[deg]	6.061
Longitude of Ascending Node, Ω_G	[deg]	185.646
Argument of perigee, ω	[deg]	180.071
True Anomaly, θ	[deg]	35.015
Time from lift-off, t_i	[s]	1689
$v_\pi - v_{esc}$	[m/s]	-27.93

3.1.4 Perigee Velocity Correction

Besides the maximum Sun-spacecraft-Earth angle, also the required perigee velocity to reach L_2 is affected by the choice of the launch date. This can be seen in figure 3.3, which illustrates the evolution of the perigee velocity relative to the escape velocity over a launch window in 2020-2022. It can be seen that especially around the equinoxes there are relatively large excursions of the perigee velocity. This is caused by the Moons influence, which is more pronounced during equinox launches due to the proximity of the transfer to the Moons orbital plane. Before the Moon crosses the transfer orbit it decelerates the spacecraft, afterwards it accelerates it. The main effect is on the required perigee velocity (corresponding to apogee radius), osculating at the epoch of injection. The perigee velocity at injection has to be preprogrammed into the launcher for each launch opportunity. Since it is desired to minimise the number of different launcher programmes, it is assumed here that only one launcher programme with one fixed value for the perigee velocity ($v_\pi - v_{esc} = -27.93\, m/s$) is used as a baseline. The variation of the perigee velocity over the launch window will have to be implemented by the correction manoeuvre, which can be carried out after two days if it is combined with the launcher dispersion correction (see section 3.4).

In order to limit the size of the correction manoeuvre, the range over which the perigee velocity is allowed to vary is confined to $\pm 1.5\, m/s$. This value is taken equal to PLATO (see [3]), which has a very similar trajectory. With the margin included (see [6]) that results in $1.58\, m/s$, which is the relevant figure for the budgeting. Launch dates, for which the perigee velocity is outside the $-27.93 \pm 1.5\, m/s$ band, will have to be cut out of the launch window. For the complete 2 years, this launcher program contains 545 feasible launch dates in the course of 2 years (74.6%). In general it can be stated that if number of launcher programmes is increased, the required ΔV for the correction manoeuvre and/or the number of cut-out days can be decreased.
Once the fixed launcher program is taken as a reference, the original launch window can be interpreted in terms of closeness to the nominal insertion conditions considering the maximum correction manoeuvre-size. All darkish coloured regions of figure 3.4 have a perigee

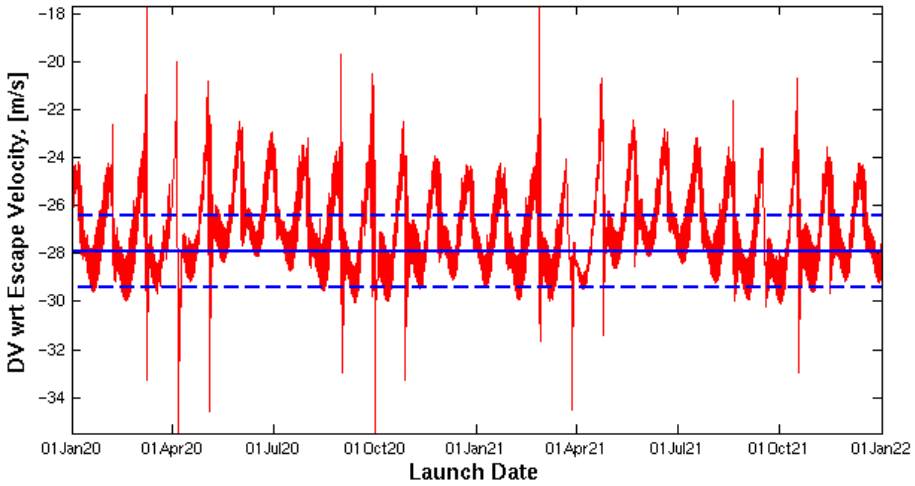

Figure 3.3: The variation of the required osculating perigee velocity relative to the escape velocity. The median value for the perigee velocity is -27.93 m/s relative to the escape velocity, pre-programmed in a fixed launcher program, with a range of 1.5 m/s, which has to be covered by a correction manoeuvre.

velocity that is close enough to the reference state ($< 1.5\,m/s$) to be covered by a spacecraft manoeuvre. What remains with a single launcher tape is a monthly launch window that lasts up to 25 days and has a daily window ranging from 1 to maximally 2 hours.

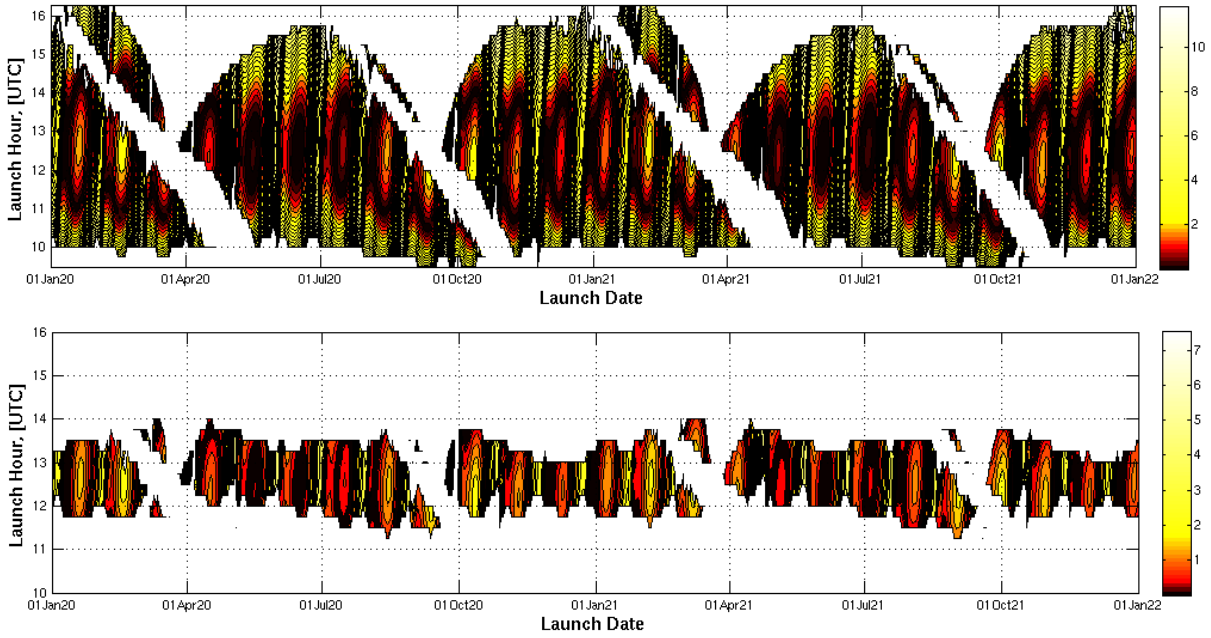

Figure 3.4: Top:the complete launch window interpreted in terms of feasible perigee correction manoeuvres. Bottom: the fixed launcher tape constraint superimposed on the launch window corresponding to a maximum amplitude of $34°$. All darkish coloured patches correspond to a perigee correction manoeuvre-size within the fixed Launcher Tape definition.

3.1.5 Fregat Disposal

Concerning the Fregat upper stage there are 2 stipulations in space law that have to be considered:

- After launch one should proceed to remove the Fregat from the highly occupied orbit regimes and eventually de-orbit it. In doing so, the risk for terrestrial casualties should also be $< 10^{-}5$
- The probability for impact with a main celestial body should be proven to be $< 10^{-}5$ over 25 years

There are 2 strategies possible for disposing of the Fregat upper stage, depending on the target orbit: de-orbiting and escaping (allowed by French Law). For either it is attempted to maximize the efficiency of the remnant AOCS propellant (42 kg).

- De-orbiting: this can be done actively and passively. For the active variant up to an apogee of 150,000 km, remnant AOCS propellant suffices: up to 70m/s). For higher apogee or direct case: performance loss. For the passive scenario, one needs to demonstrate that the atmospheric pressure reduces the perigee sufficiently to re-enter. To achieve the low casualty statistic the re-entry is traditionally done in the south pacific
- Escaping: From an apogee of 225,000 km onwards, remnant AOCS propellant suffices. For lower apogee: performance loss. In this case it can be challenging to demonstrate the required 25 years of collision-free flight with a sufficiently large confidence interval

3.2 Geometric Attitude Constraint

As was mentioned before, this constraint is raised by the missing mirror cover and may prehibit a certain class of transfers to L_2 . The actual constraint means that no bright body can enter the FOV of the telescope, which is defined as a cone with half-cone angle of 20° around the viewing axis oriented along the longitudinal axis of the spacecraft. Since no detailed AOCS design is currently available, it can only be hypothesized that the general thrust direction is along the LOS of the telescope. Therefore, when making this assumption, both the LOS and thrust direction have to be kept out of the [0;20°] and [160°;180°] angles with the Sun direction. This critical situation can only occur during the transfer since the nominal orientation of the telescope during the operational phase is (close enough to) perpendicular to the sun direction. Since at the moment of the first TCM, the velocity vector lies close to the unstable velocity direction, the thrust direction can be approximated well with the tangential direction. Figure 3.5 shows typical evolutions for the tangential direction for transfers at different launch times of the same day. Now, the transfers could be selected such that this geometric constraint is not violated, but another option is to assume a suboptimal thrust direction for the TCMs. That approach is valid since only the component of the manoeuvre ΔV along the unstable direction is fixed. The other component is considered a loss, but does not prevent the spacecraft to stay inside the stable manifold. Although figure 3.5 shows that there is a violation of the attitude constraint for some cases, the sub-optimal thrust direction can be chosen to lay outside the FOV, whereas the loss behaves according to the cosine of the angle. If the angle amounts to 10°, larger than any case in the figure, the loss is quantified to merely 1.5%, which falls within the margin on the required manoeuvre budgets. The removal of those transfers from the valid launch window thus depends on the weight that is given to the losses.

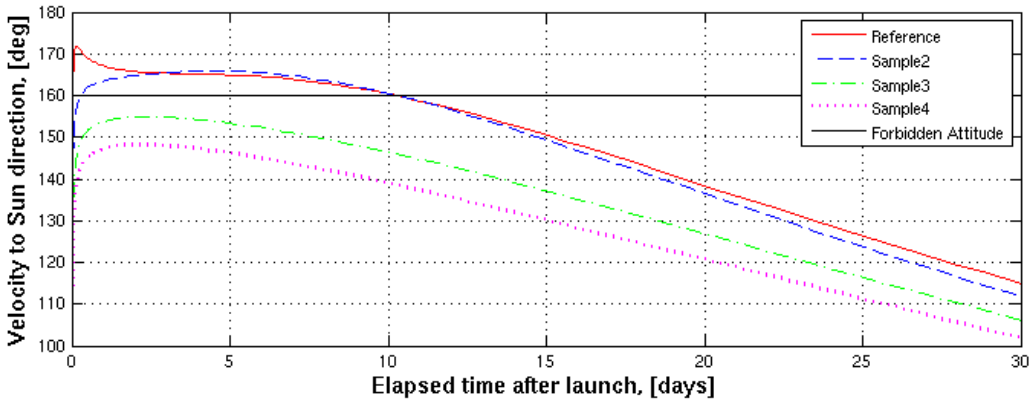

Figure 3.5: The evolution of the velocity to Sun direction during the transfer for various launch hours on the same day. Launches are on 1-1-2020 at 11:30, 12:30, 15:30 and 16:00.

3.3 Mission Event Sequence During Transfer

The mission event sequence during transfer is driven by the requirements of the navigation only (in this early stage of the project). The launch by the Soyuz Fregat MT will inject the spacecraft directly into the transfer trajectory towards L_2 . While the timing for the commissioning and deployment is not strongly time-critical, the performance of trajectory correction manoeuvres is. As is discussed below, the errors and biases in the spacecraft state vector at injection will increase over time, so that the correction manoeuvres become more demanding in ΔV if they are performed at a later time. On the other hand, there must be enough time to measure the errors by tracking the spacecraft with the ground-station. For those reasons it is intended here to provide a first framework of the mission event sequence as an overview. Operational requirements for the deployment or the commissioning might change the detailed sequence, but the general structure should be as follows:

- The launch and early operations phase (LEOP) extends from launch to just after the first correction manoeuvre
- After injection, spacecraft tracking data is collected for up to two days used to determine the spacecraft state vector
- During tracking, initial commissioning is performed
- At the latest on day 2 after launch a correction manoeuvre is performed in order to achieve the required perigee velocity and correct the dispersion created by the launcher. It is assumed here that the thrust is sufficient to deliver the required ΔV within less than 2 hrs, so that the manoeuvre can be assumed to be impulsive
- After the first correction manoeuvre until day 10 after the launch, tracking data will be collected in order to determine the error in the that manoeuvre as well as any dynamic perturbations
- Further commissioning can be performed in the period between day 2 and day 10
- On day 5 and 10 a second and third correction manoeuvre is budgeted and scheduled, which corrects the error of the previous one(s) and puts the spacecraft stack precisely on the stable manifold of a large amplitude orbit around L_2 . That these manoeuvres

are scheduled does not mean they will take place. It can only be stated that these manoeuvres are necessary with a statistical probability, as will be shown later.

- After the third correction manoeuvre, the deployment of the telescope is performed
- The spacecraft performs final commissioning, after which the science operations commence

Table 3.3: Sequence of events during transfer.

Elapsed Time from Lift-off	Comment
L + 1689 s	Satellite separation Satellite wake-up **Start of** check-out, tracking, commissioning campaign Orbit determination, TCM command generation and Command uplinking
L + 1 day	Opening of TCM1 window
L + 2 days	Closing of TCM1 window
L + 5 days	TCM2
L + 10 days	TCM3
L + 30 days	Arrival at L_2 vicinity
L + 104 days	End of Transfer deterministic ΔV-free insertion in operational orbit. begin of Science Phase

3.4 Launcher Dispersion Correction Manoeuvres

3.4.1 Manoeuvre Timing

The transfer orbit is chosen such that the spacecraft enters a ΔV-free manifold towards the L_2 region and is automatically (free from any deterministic manoeuvres) inserted in a Quasi Halo orbit around L_2 . This is also called the *stable manifold* and is a very small region in the vicinity of the earth. If not inserted precisely into this manifold a small velocity residual may already be enough to diverge from the manifold. Due to this diverging behaviour, the correction becomes more expensive with time. This non-linear effect is expressed as a penalty factor. At the moment of the virtual perigee passage this factor is 1 (no additional cost), but steeply increases to e.g. a value of 8 at day 2 and 20 at day 10.

This creates a situation in which immediately after the separation of the spacecraft from the Fregat upper stage a tight schedule has to be worked through, such that the TCM can be performed as early as possible to minimise the ΔV cost and maximise the payload mass: commissioning, engine calibration (possibly even skipped), orbit determination and command generation and uplinking. For the direct insertion this manoeuvre cannot be performed before day 1 and normally is budgeted for day 2 (highest penalty factor). For the actual ΔV budgets corresponding to the penalised manoeuvre size, please be referred to the conclusions. Logically, this manoeuvre becomes critical and for certain regimes of manoeuvre underperformances the mission is unrecoverable. The TCM1 maoeuvres aims at resolving:

- The osculating perigee velocity, previously described in section 3.1.4
- The launcher dispersion, see following section

3.4.2 Launcher Dispersion

The insertion state of the spacecraft will be different from the nominal state. This behaviour depends on the ascent trajectory and the covariance matrix. The dispersion ellipse at injection describes the set of initial states may occur. The spacecraft itself has to correct for error. Of course that can only be done after intensive orbit determination, which still will have a finite accuracy. Also the manoeuvre execution will not be perfect; therefore the combined effect is that there is still an unresolved error, which has to be corrected later on.

From the available Soyuz MT correlation matrix and standard deviations for insertion in an L_2 orbit, see [7], the dispersion or covariance matrix can be reconstructed. This matrix will be used in the next section to assess the dispersion correction manoeuvres.

3.4.3 Numerical Simulation of Launcher Dispersion

Due to the different initial state of the spacecraft, which is a consequence of the limited launcher injection accuracy, the spacecraft is most likely not located anymore on a deterministic ΔV-free transfer towards L_2 . Therefore a correction is required to either bring the satellite back to the nominal path or to navigate to a new transfer along the stable manifold. Due to practical constraints the first manoeuvre cannot take place before a full day after launch, as illustrated in section 3.3. This statistical analysis is performed by a Monte carlo simulation that propagates the erroneous injection state, calculates and alternative transfer and navigates towards the new trajectory by means of a series of manoeuvres. The numerical simulation takes into account dynamical model noise, simulates the measurements and accomodates the limited measurement accuracy by applying an additional spectral noise, manoeuvre execution errors, ground station location biases and several perturbations (a.o. solar radiation pressure and third body perturbation). The reason for a series of manoeuvres in the transfer navigation is dual: firstly, given that the manoeuvre execution errors are finite, other manoeuvres are required to compensate the undesired effect of the previous ones. Secondly, increasing the number of manoeuvres allows for a higher degree of optimisation of the navigation scheme.

For the sake of completeness, the full set of input data for this simulation is contained in table 3.4. The values are chosen generically, rather conservative, and are based on the experience of previous projects. The result is a table with statistical information about the 3 LDCM's and is contained in table 3.5. Please note that these results directly follow from the assumptions made in the table, specify geometric ΔV, have no limitation on the thrust direction, did not model gravity losses and contain no margins. The relevant numbers will be extracted in the chapter: *Conlusions*.

Table 3.4: Summary of simulation input data, orbit determination and manoeuvre execution accuracy, spectral noise definition during the transfer phase (all values are $1-\sigma$).

Quantity	Value
perturbing bodies apart from Sun and Moon	Jupiter, Saturn
solar radiation pressure flag	0
manoeuvre execution epochs	day 2, 5, 10
ground-station in transfer phase	Cebreros
cut-off elevation	10.0°
frequency of Doppler measurements	once every 10 min
frequency of range measurements	once per pass
range measurement random error	20 m
range measurement consider bias	20 m
Doppler measurement random error	0.03 $mm\,s^{-1}$
Doppler measurement consider bias	$<$ 0.001 $mm\,s^{-1}$
station coordinates in equator plane	30 cm
station coordinates out of equator plane	1 m
precision in correction ΔV magnitude ($>$ 20 $cm\,s^{-1}$)	3%
precision in correction ΔV direction ($>$ 20 $cm\,s^{-1}$)	2.5°
precision in correction ΔV magnitude ($<$ 20 $cm\,s^{-1}$)	4 $mm\,s^{-1}$
precision in correction ΔV direction ($<$ 20 $cm\,s^{-1}$)	5°
autocorrel. time for filter model s/c non-grav. acc. 1	1
autocorrel. time for filter model s/c non-grav. acc. 2	5
autocorrel. time for filter model s/c non-grav. acc. 3	10
autocorrel. time for real world s/c non-grav. acc. 1	1
autocorrel. time for real world s/c non-grav. acc. 2	5
autocorrel. time for real world s/c non-grav. acc. 3	10
standard deviat. for filter model s/c non-grav. acc. 1	10^{-12}
standard deviat. for filter model s/c non-grav. acc. 2	10^{-12}
standard deviat. for filter model s/c non-grav. acc. 3	10^{-12}
standard deviat. for real world s/c non-grav. acc. 1	10^{-12}
standard deviat. for real world s/c non-grav. acc. 2	10^{-12}
standard deviat. for real world s/c non-grav. acc. 3	10^{-12}
flag for solar radiation pressure error	1
autocorrel. time for solar radiation pressure error	1
standard deviat. for solar radiation pressure error	10

3.5 Transfer Navigation: Trajectory Correction Manoeuvres

The complete transfer navigation or transfer orbit maintenance consists of navigating the spacecraft onto a stable manifold towards L_2 . The required manoeuvres during this phase need to account for all errors that are introduced so far:

- The perigee velocity error: due to the daily and monthly variations in required orbital

Table 3.5: Results of Monte Carlo analysis simulating a series of launcher dispersion correction manoeuvres during transfer towards L_2 .

		Manoeuvre Size $[m/s]$			
LDCM	Timing	Mean ΔV	St. Dev.	95%	99%
1	Day 2	22.52	7.41	35.09	39.06
2	Day 5	00.85	0.74	02.33	03.26
3	Day 10	00.03	0.04	00.12	00.17
	Total	23.41	7.72	36.32	42.49

energy and the definition of a fixed launcher tape, see 3.1.4

- The velocity error at injection: due to the launcher dispersion, see 3.4

The budget for the perigee velocity correction manoeuvre has been specified at the virtual perigee above, but of course it cannot be performed at that moment in the real world. It is effectuated at the same time as the LDCM and therefore will take place at Day 2. As illustrated in section 3.4.1 unstable dynamical behaviour will affect the trajectory such that there is an amplification factor on that budget that grows in time. The penalty factor for day 2 is 8, hence the 12.6 m/s for the PVCM.

Table 3.6: Summary for the manoeuvre sizes of the Trajectory Manoeuvre Correction Manoeuvres during transfer towards L_2 for 99% of the cases.

Man #	Timing	LDCM $[m/s]$	PVCM $[m/s]$	TCM $[m/s]$	TCM Direction
1	Day 2	41.01	12.6	53.61	tangential
2	Day 5	3.42	0.0	3.42	unstable direction
3	Day 10	0.18	0.0	0.18	unstable direction
	Total	44.61	12.6	57.21	

The perigee velocity error represents a difference in orbital energy that has to be compensated with the PVCM. On an non-return trajectory that correction is more efficient the closer to the perigee, but should always be imparted tangentially (for the efficiency). Although it is not shown here, it can be demonstrated that the optimal manoeuvre direction is the velocity direction during the early stage of the transfer and later on (e.g. from day 5 onwards) that is the unstable direction. This direction is a result from the linearised dynamics and therefore loses it's validity the further away from L_2 . In general it can be stated that the unstable direction lays in the ecliptic plane tilted $+28.6°$ away from the Sun-Earth axis. This implies that the forbidden attitude is not endangered for the day 5 and 10 manoeuvres, while the impact on the ΔV budget for day 2 due to the cosine loss, is always minimal as shown before.

A final important remark goes to the criticality of TCM1. A simple back-of-the-envelope calculation show that if the TCM1 cannot be performed punctually at day 2 but at day 3 or 4, the required ΔV budget quickly increases by 24% or 42%. Not only the required propellant mass for the TCM's will rise, but also the budget for the contingency scenarios. In case of an underperformance of the TCM, it will gradually become more and more difficult to recover the mission, if possible at all. For the HEO scenario an engine misfiring or underperformance can be dealt with in a rather inexpensive manner.

4 Conclusions

In this Mission analysis guidelines document it is shown that, from the mission analysis point of view, EChO is a feasible mission. In the near future the developments in the design of the observation (attitude) strategy, communications, propulsion and AOCS systems may have affect the launch window, transfer navigation, operational orbit and orbit maintenance. The impact has to be assessed and processed in a future CReMA. For the moment being the mission analysis result are summarised here.

4.1 Alternative Mission Scenario

As an alternative mission scenario (see also appendix A) there is the possibility to insert the spacecraft into a HEO. At the next perigee passage the spacecraft would perform an (near-)escape manoeuvre to insert itself in a transfer towards L_2 . There are two clear advantages: first, there is more time to prepare for the escape manoeuvre and second: there is no penalty factor that increases the ΔV budget for that manoeuvre as is the case for the direct insertion scenario. The combination of the launcher performance with the LEOP and transfer manoeuvres as a function of the apogee radius of the insertion orbit, concludes in a graph that presents the payload mass that can be inserted by the launcher in an orbit around L_2 . In this graph the gravity loss, for the escape manoeuvre in the HEO scenario, has been taken into account. This explains the strong performance loss for low HEO apogea due to the low available thrust and Isp (gravity loss up to 140%). The break-even point between both options lies around an approximate HEO apogee radius of $250,000\,km$. The possible mass gain amounts a maximum of roughly $50\,kg$, while for reasonable regimes of HEO apogee altitude, the potential mass gain is less (around $20\,kg$). The direct insertion is chosen for the

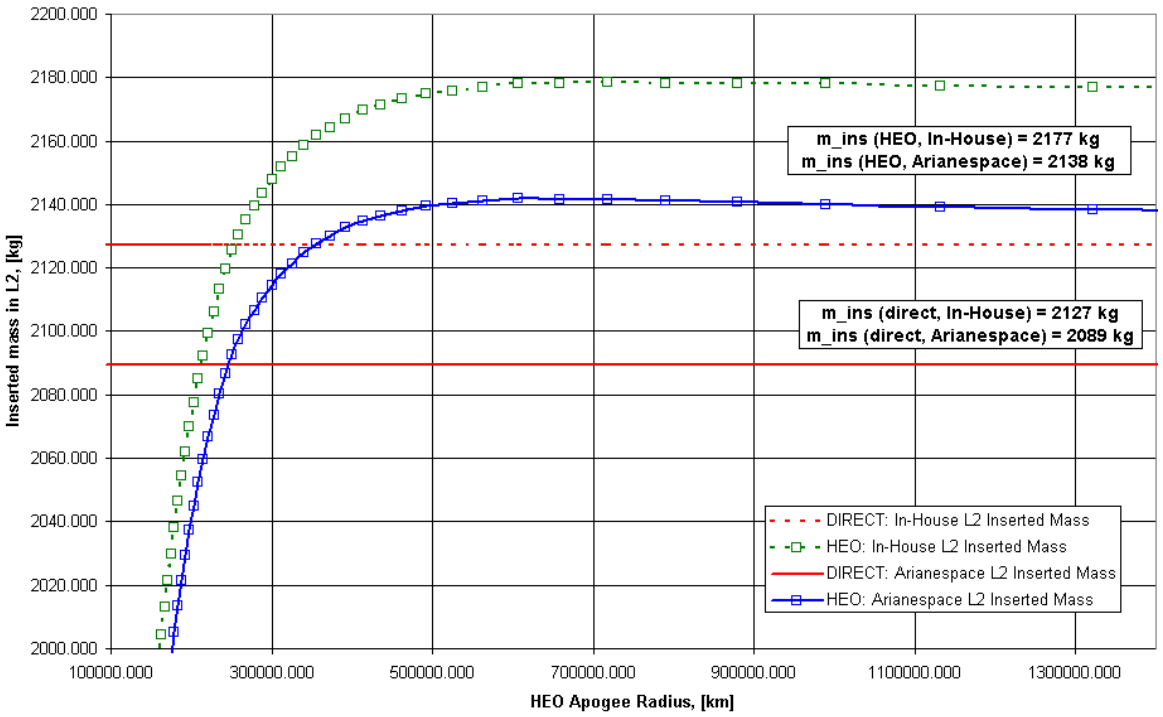

Figure 4.1: Mass performance at the end of the transfer phase for both scenarios. The curves include: launcher performance, gravity loss for escape manoeuvre, Fregat escape, ideal TCM1 (launcher dispersion correction and perigee velocity correction) and all margins. The TCM1 is executed at day2 for the direct ascent and at perigee for the HEO case.

following reasons:

- The CDF design is far from mass critical and the final mass performance for the HEO scenario is only slightly more,
- The LEOP duration increases by maximally 25 days for the HEO scenario
- To cope with the larger ΔV budget (as a function of the intermediate orbits apogee height), the spacecraft may have to be equipped with a second tank,
- The criticality of the day 2 TCM is relative, also other missions have done it before: Herschel/Plank and Gaia and PLATO have it baselined as well,
- The absence of the mirror cover or mechanism would mean that also in the case of the intermediate HEO, the Earth albedo light may enter the telescope. This is because for a low perigee altitude (200 km) the Earth disc is larger than a half cone angle of 70°. With the current thruster decomposition the orientation of the telescope will be along the velocity direction since the escape manoeuvre is performed tangentially to the orbit. The Earth albedo was later also constrained from entering the forbidden attitude. During the HEO orbit an attitude manoeuvre would be required to point the spacecraft to a dark region.
- The direct launch gives the lowest performance of both and offers the least complexity, therefore it is chosen as the sizing case.

4.2 Launch window

In the calculation of the launch window for 2020-2022 there were only 2 constraints to be taken into account: firstly, the orbit size has to satisfy the following condition $max(SSCE) < 34°$ and secondly both the transfer and the operational orbit have to be free from eclipses for the whole duration of the mission. From the results it is seen that there is a nearly continous launch window, of about 3 weeks per month, with a larger outage percentage during the equinoxes. In those periods the probability for an eclipse in the science phase of the mission increases due to the initial proximity to the ecliptic of the spacecraft at injection. The impact of the maximum amplitude is manifested by the reduction of the daily launch window only solutions of $max(SSCE) < 34°$ are possible for launches that occur between 11:20 and 14:00 UTC. The smallest amplitude orbits are obtained for launches at 12:30 UTC. Although there exists a daily window in which both the transfer and the orbit may comply all constraints, they may exhibit different longterm behaviour. That is a consequence of the varying RAAN at launch, which translates into the daily launch time.

4.3 Operational Orbit

The properties of the operational orbit cannot be captured with a single set of elements, simply because there are families of possible trajectories with vague boundaries between them. It is clear that the quasi halo orbit type is favoured due to the proximity of the in- and out-of plane oscillation periods which results in a relatively steady orbital behaviour. This aspect may be benign for the communication system design, since the SSCE angle varies as few as possible. When the relation between both motions is not imposed anymore still suitable solutions are found, but the SSCE variation will be larger, which may require a pointing mechanism for the on-board antenna, depending on the attitude model.

Table 4.1: Summary for orbit maintenance budget as a function of lifetime extension, including margin.

ΔV	Lifetime extension, $[yrs]$				
	1	2	3	4	5
Nominal Phase, $[m/s]$	30				
Extension Phase, $[m/s]$	6	12	18	24	30

The amplitude in all three directions, which is the maximum excursion from L_2, is constrained to $< 34°$, which is approximately $1\ 10^6\ km$. The reason is that with increasing orbit size, the quasi-halo criterion is more difficult to impose and secondly the dynamics cause a larger orbit maintenance cost (when the amplitude becomes several millions of kilometers.)

Due to the lack of input data related to the propulsion and the AOCS systems, only the geometric ΔV for the orbit maintenance can be estimated. The numerical analysis could not be performed within the frame of the MAG for several reasons, but will constitue an important part in a later CReMA. So far, the thruster collocation on the spacecraft has been compared to previous missions. From that a conservative estimate of the required geometric ΔV budget is derived. The budget is set to $6\,m/s/year$ including margin. That gives the budget for the nominal and extended mission, as in table 4.1.

4.4 Launch

The Soyuz Fregat MT launch from Kourou with direct injection into the transfer towards L_2 has been designed such to maximise the launch performance. The nominal orbital elements at injection are: $r_\pi = 335.25\,km$, $e = 0.9906$, $i = 6.061°$, the argument of the ascending node with respect to Greenwhich $\Omega_G = 185.646°$, the argument of perigee $\omega = 180.071°$ and $\theta = 35.015°$. From the launch window it appeared that there are plenty of launch oportunities centered around 1230 UTC. That means that a single flight program suffices to be contracted with the launcher authority. That flight program allows for a variation of $1.5\,m/s$ in the perigee velocity due to daily and monthly variations, that can still be corrected later on. The mean value for the difference between the actual perigee velocity and the escape velocity, which defines the flight program lies at $-27.93\,m/s$. For these conditions the launch payload mass is $2145\,kg$, which includes the adapter and margin.

4.5 Transfer

The injection of the spacecraft by the launcher has only a finite accuracy. In combination with the variation of the orbital energy of the insertion orbit (perigee velocity error) this error defines a set of initial states from where the spacecraft needs to be guided towards L_2 . For that purpose a series of manoeuvres is scheduled to correct the velocity vector. The distinction is made between the Launcher Dispersion Correction (LDCM) and the Perigee Velocity Correction (PVCM). The values are summarised for both scenarios in table 4.2, where N/S stands for *not simulated*. These values have merely been estimated, since the HEO scenario is only an alternative solution.

Table 4.2: Summary of TCM budget for both options, including margin.

Man #	Timing	LDCM $[m/s]$	PVCM $[m/s]$	TCM $[m/s]$	TCM Direction
HEO					
1	Perigee	5.58	1.58	7.26	tangential
2	Day 5	N/S	N/S	N/S	unstable direction
3	Day10	N/S	N/S	N/S	unstable direction
	Total			**7.26**	
Direct					
1	Day 2	41.01	12.6	53.61	tangential
2	Day 5	3.42	N/S	3.42	unstable direction
3	Day 10	0.18	N/S	0.18	unstable direction
	Total	44.61	12.6	**57.21**	

The total trajectory correction manoeuvre at the perigee is therefore set to $7.26\,m/s$. Note that only in the HEO scenario the manoeuvre can actually be executed at the perigee, being after a complete orbital revolution. For the nominal direct insertion that manoeuvre takes place no later than day 2, but by then the required total transfer navigation budget will have inreased to $57.21\,m/s$. This value expresses the ΔV budget for a 99% confidence interval and is the result from a full Monte Carlo analysis.

4.6 ΔV Breakdown

Table 4.3 summarises the required ΔV for the direct insertion baseline both in the transfer and the operational orbit.

Table 4.3: Direct Insertion ΔV budget breakdown.

Event	Geometric ΔV, $[m/s]$
TCM1	53.61
TCM2	3.42
TCM3	0.18
Orbit Maintenance	36
Total	93.21

A Transfer Alternative: Launch into HEO

However, there are two different options available for this L_2 orbit: a small amplitude orbit and a large amplitude orbit. Also for the launcher injection strategy, different options exist: launching directly towards L_2 , or using a parking orbit and then use the spacecraft's propulsion system for the injection into the L_2 transfer orbit. For the direct insertion it is the Fregat upper stage that provides the required ΔV to put the spacecraft in the transfer trajectory towards L_2 , while for the HEO scenario the Fregat inserts the EChO spacecraft into a high elliptical orbit, with a manoeuvre at the following perigee. Depending on the orbit geometry with respect to the Sun-Earth axis, the actual Moon position and the size of the HEO, gravitational third body perturbations will play an important role. Typically these perturbations produce changes in the perigee radius. Therefore a manoeuvre may be required at the apogee to compensate this lowering effect and to guarantee the desired conditions at the moment of the next perigee burn or escape manoeuvre. The location of the perigee, and therefore the in-plane orientation of the orbit, will determine the perigee manoeuvre orientation and consequently also the amplitude of the L_2 orbit. For the quantification of the trade-off later on, it is assumed that the geometry of the HEO is such that there is no perigee lowering (due to third body perturbations). With respect to the solar gravitational perturbation that implies that the apsis line coincides with the sun-Earth axis.

Table A.1 shows a summary of the options plus the advantages (in green) and disadvantages (in red) used for the orbit trade-off. A large amplitude L_2 orbit was chosen for the following reasons:

- A large amplitude orbit drastically lowers the total ΔV
- The low data rate allows for data downlink twice a week
- The CDF design allows, with the required observations duty cycle and ΔV budget, spacecraft pointing instead of a risky/costly antenna pointing mechanism.

The trade-off between both launcher scenarios had to be quantified in order to make a founded decision. Therefore, in the following paragraphs the implications for the HEO scenario are commented as the counterpart of the content of this MAG, which is dedicated to the direct insertion scenario.

A.1 Apogee Raising Manoeuvre from HEO

This manoeuvre is only required for the HEO scenario and replaces one of the functionalities of the Fregat stage. The most important benefit is that the in section 3.4.1 described penalty factor is 1 for a manoeuvre at the perigee instead of 8 at day 2. That results in a lower ΔV budget. The largest disadvantage is that the current spacecraft design does not have a high thrust propulsion module, but instead a mono-propellant system with $2x20\,N$ thrusters and a lower specific impulse, compared to the Fregat. That means that the large manoeuvre, come together with extreme gravity losses. Other benefits are: firstly that the criticality of the day 2 manoeuvre is relaxed. Depending on the apogee radius of the HEO orbit the time to the first manoeuvre will be considerably larger. For example: if the apogee radius is $200,000\,km$ the period will be approximately 10 days. In case there is no need for a perigee raising manoeuvre (see [1]), the first manoeuvre will be the escape manoeuvre after 10 days, which creates a large window for ground operations to prepare for the manoeuvre. Secondly, for the HEO option the staging effect is exploited, which creates a potential mass saving, whereas the Fregat also has to propel itself (roughly 1 ton dry mass).

Table A.1: Orbit options trade-off table.

	Large Amplitude	Small Amplitude
HEO	No insertion ΔV	High insertion ΔV
	May need antenna repointing	No antenna repointing
	Engine calibration possible	Engine calibration possible
	Relaxes launcher dispersion manoeuvre	Relaxes launcher dispersion manoeuvre
	Small ΔV budget for TCM's	Small ΔV budget for TCM's
	Escape manoeuvre done by s/c	Escape manoeuvre done by s/c
	May need mirror cover, shutter mechanism	May need mirror cover, shutter mechanism
DI	No insertion ΔV	High insertion ΔV
	May need antenna repointing	No antenna repointing
	Tight schedule for launcher dispersion manoeuvre	Tight schedule for launcher dispersion manoeuvre
	High ΔV budget for TCM's	High ΔV budget for TCM's
	Escape manoeuvre by Fregat	Escape manoeuvre by Fregat
	No need for mirror cover	No need for mirror cover

A.2 Trajectory Correction Manoeuvre

For the HEO case there are 2 clear advantages. Firstly, the performance is not affected by the previously mentioned penalty factor, since the TCM can be executed together with the escape manoeuvre at the perigee. Secondly, the manoeuvre takes place after a complete revolution, meaning that there is plenty of time for commissioning, engine calibration, orbit determination and command generation. For the direct insertion, however, this manoeuvre cannot be performed before day 1 and normally is calculated at day 2.

A.3 Extended LEOP Duration

In order to profit from the benefits that an intermediate HEO provides, the LEOP duration is extended by an orbital period. The period as a function of the apogee radius is given in figure A.1. In order to avoid large performance losses, large duration extensions and (not investigated) third body perturbations on the perigee, the HEO apogee is bounded between $270,000$ - $350,000\,km$, which corresponds to a period of 15 - 24 days. The apogee also lies high above the Van Allen belts, so no excessive radiation exposure is suffered.

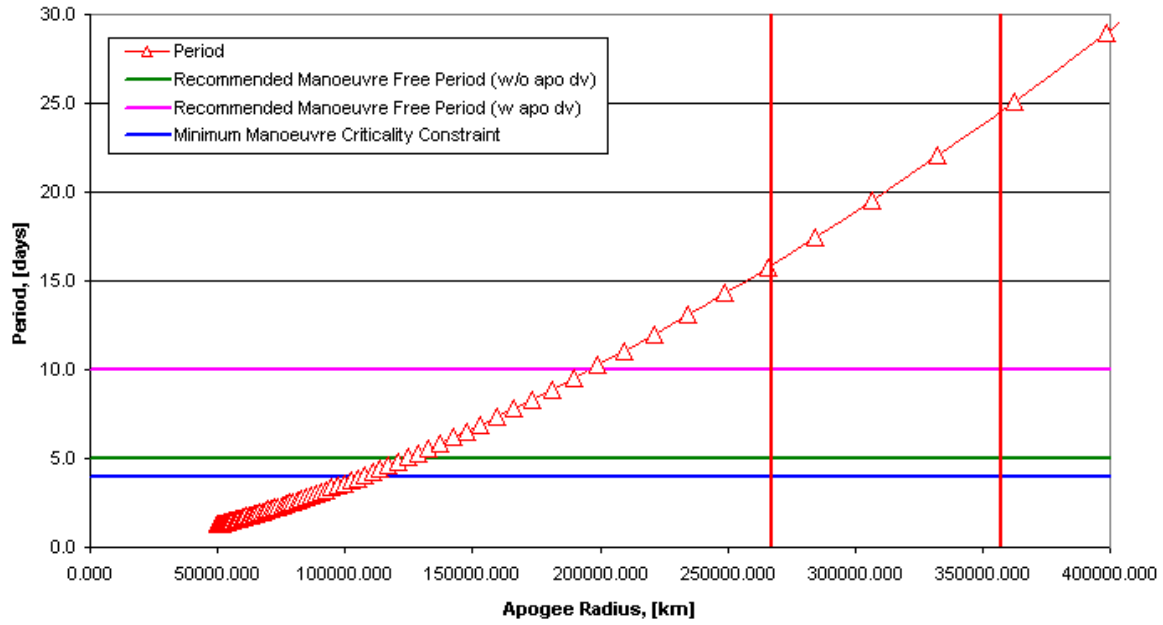

Figure A.1: Period duration as a function of the apogee radius. Also indicated are: the mass performance break-even point and the radius of the Moon orbit.

References

[1] A. Pickering. Echo exoplanet characterisaton observatory. CDF Study Report CDF-118(A), ESA, ESA/ESTEC, Postbus 299, 2200 AG Noordwijk, The Netherlands, July 2011.

[2] A. Yanez M. Hechler. Herschel/planck: Consolidated report on mission analysis, issue 3, revision 1. WP PT-MA-RP-0010-OPS-GMA, ESOC, January 2006.

[3] M. Landgraf F. Renk. Plato: Consolidated report on mission analysis, issue 1, revision 3. WP WP561, ESOC, November 2010.

[4] ECHO Team. Echo mission requirements document. MRD Issue 1.1, ESA/ESTEC, June 2011.

[5] M. Hechler J. P. Mellado. Gaia mission analysis, eclipses by the moon. WP WP499, ESOC, September 2006.

[6] Margin philosophy for science assessment studies. TN SCI-PA/2007/022/, ESA, 2007.

[7] A. Macaire. Lunar lander: Soyuz st-b fregat mt, trajectory and performance - feasibility study - final meeting. Presentation AE/DP/SY/LM N11-133, Arianespace, May 2011.